

Temperature dependence of the magnetic excitations in iron*

J. W. Lynn^{††}

Solid State Division, Oak Ridge National Laboratory, Oak Ridge, Tennessee 37830

(Received 9 September 1974)

The neutron coherent inelastic-scattering technique has been used to study the temperature dependence of the magnetic excitations in iron from room temperature to well above the ferromagnetic transition temperature. Most of the measurements were taken on a large single crystal of ^{54}Fe (12-at.% Si), although a less extensive set of data was obtained with a single crystal of pure iron. In contrast to the behavior previously observed in the small-wave-vector region, we find that the spin waves at larger values of \vec{q} are only moderately renormalized up to T_C , and persist as excitations up to the highest temperature measured ($\sim 1.4T_C$). No further renormalization of the dispersion relation is observed above T_C . Measurements of the spin-wave linewidths show that as the temperature increases to T_C the widths rapidly increase, but above T_C no additional broadening occurs. In the paramagnetic phase the ratios of the energy widths divided by the excitation energies for $E \gtrsim 8$ meV are found to be less than one ($\Delta E/E < 1$), which has been used as the criterion for the definition of a spin-wave excitation. As the energy decreases below ~ 8 meV, the scattering evolves continuously into the critical scattering around the origin ($\vec{q} = 0$, $\omega = 0$), whereas with increasing energy $\Delta E/E$ decreases. The dynamical correlation range corresponds to a sphere with a diameter ~ 10 Å, and this correlation range is, within experimental error, independent of the temperature. The over-all spin-wave intensities are reduced at elevated temperatures, but the abrupt decrease in the spin-wave intensity at high energies, interpreted in terms of the band model of magnetism as the intersection of the spin-wave spectrum with the Stoner continuum of spin-flip excitations, is found to be independent of the temperature. The spin-wave energies, as well as the linewidths, are isotropic in \vec{q} over the entire temperature range covered, and no interaction of the spin waves with the phonons is observed. These experimental results are in disagreement with present theoretical estimates of the generalized susceptibility at elevated temperatures.

I. INTRODUCTION

The magnetic properties of the 3d ferromagnetic metals have been under intensive investigation for many years. In fact, they have probably been studied by more researchers and with a wider variety of techniques than any other magnetic materials. The experimental evidence has established that the *d* electrons in these metals occupy relatively narrow energy bands which are itinerant in character, although the strong intraatomic electron correlations present inevitably give rise to some properties which are localized in nature.¹ Thus at low temperatures both the "single-particle" properties (such as Fermi surfaces, photoemission spectra, etc.) as well as the collective excitations of these ferromagnets are best described by calculations which are based on "tight-binding" band structures in which the electron correlations are handled as accurately as possible. However, the nature of the band structure and the electron correlations at elevated temperatures is not yet fully understood.²

The quantity of fundamental importance in understanding these magnetic systems is the wave-vector- and frequency-dependent generalized magnetic susceptibility $\chi(\vec{q}, \omega)$. This is because χ contains a complete description of the magnetic excitation spectrum of the system; so, with a knowledge of $\chi(\vec{q}, \omega)$, the (linear) response of the system to any

magnetic disturbance can be found. This dynamic susceptibility is directly related to the coherent magnetic inelastic scattering of neutrons, which is in fact the only experimental technique available to measure both the wave-vector and frequency dependence of $\chi(\vec{q}, \omega)$.

The scattering of thermal neutrons has already been used extensively to study the magnetic properties of iron. In particular, the techniques of small-angle scattering, diffuse scattering, and the "diffraction method" have been employed to measure³⁻⁷ the long-wave-length spin dynamics. From these experiments it was inferred that at low temperatures the spin waves are isotropic in \vec{q} , with the dispersion relation being given approximately by $E = D|\vec{q}|^2$. Above the ferromagnetic transition temperature, considerable information was obtained about the nature of the diffusive modes which revealed the presence of strong short-range spin correlations. Unfortunately, however, the interpretation of these types of experiments, in which the directions but not the energies of the scattered neutrons are measured, depends on a number of assumptions.

With the advent of high-flux reactors, $\chi(\vec{q}, \omega)$ could be determined directly. Collins *et al.*⁸ and Boronkay and Collins⁹ have used the triple-axis technique to measure the critical scattering in detail. They found that in the small-wave-vector low-energy region the spin dynamics are well described

by dynamic scaling theory. The spin-wave stiffness parameter $D(T)$ was found to follow a power law of the reduced temperature, with the spin waves becoming overcritically damped just below T_C . However, no central diffusive mode was observed below T_C in Fe, in contrast to some antiferromagnets, and there was evidence that a highly damped propagating mode existed in the "transition" region. Furthermore, the spin-wave damping at the highest wave vector measured (0.26 \AA^{-1}) was found to be anomalous, and this anomaly was tentatively attributed to a conduction-electron screening effect.

In addition to these temperature-dependent measurements, the spin-wave part of $\chi(\vec{q}, \omega)$ has been measured at room temperature in detail. However, the spin-wave dispersion relations in the 3d metals are very steep; so at larger wave vectors the energies become rather high for neutron-scattering techniques to measure. Collins *et al.*⁸ measured a portion of the dispersion relation and found that it was isotropic in \vec{q} up to the highest spin-wave energies they could measure ($\sim 70 \text{ meV}$). This energy corresponds to a \vec{q} vector which is about 40% of the way to the zone boundary. Approximating the dispersion relation in this wave-vector region by

$$\hbar\omega_{\vec{q}} = D|\vec{q}|^2(1 - \beta|\vec{q}|^2), \quad (1)$$

they obtained values of $D = 281 \text{ meV \AA}^2$ and $\beta = 0.96 \text{ \AA}^2$. They concluded that for the Heisenberg model to fit the dispersion relation the exchange interaction would have to be of very long range. Mook and Nicklow¹⁰ were able to extend the room-temperature measurements to higher spin-wave energies on an ^{54}Fe (4 at. % Si) sample. The spin-wave intensities measured as a function of energy were found to decrease slowly with increasing energy up to $\sim 85 \text{ meV}$ and then drop rapidly by more than an order of magnitude, becoming unobservable. This rapid decrease in intensity occurred at different energies in different symmetry directions and was interpreted in terms of the band model of ferromagnetism as the intersection of the spin-wave spectrum with the Stoner continuum of single-particle spin-flip excitations.

With increasing temperature it was expected theoretically that the splitting between the spin-up and spin-down electron energy bands would vary in a manner proportional to the magnetization, and hence the region of high density of Stoner states would decrease in energy. In order to check this conjecture, a study was undertaken of the temperature dependence of the spin-wave spectrum in nickel, in which a similar fall off of the spin-wave intensity at high energies had been observed.¹¹ It was found¹² that not only did well-defined spin-wave excitations exist above the ferromagnetic

transition temperature, but also the energy at which the spin-wave modes disappeared was temperature independent. In fact, except for very small wave vectors, the whole spin-wave spectrum changed remarkably little between 4.2 and 715 °K, which is 86 °K above T_C .

In view of these results it was clear that a comprehensive investigation of the temperature dependence of the spin correlations in the ferromagnetic 3d elements would be interesting. The present article reports the first general determination of $\chi(\vec{q}, \omega)$ as a function of temperature for iron, with particular attention being given to the scattering outside the critical region. It should be noted that preliminary accounts of the data have been briefly reported previously.¹³

II. THEORY

The spin-only¹⁴ magnetic cross section for unpolarized neutrons can be written in terms of the generalized susceptibility of the electrons as¹⁵

$$\begin{aligned} \frac{d^2\sigma}{d\Omega d\omega} = & \left(\frac{\gamma e^2}{m_e c^2} \right)^2 \frac{N\hbar}{\pi(g\mu_B)^2} \frac{k'}{k} |F(\vec{K})|^2 e^{-2W(\vec{K})} (1 + f^-) \\ & \times \{ (1 - \kappa_z^2) \text{Im}[\chi^{zz}(\vec{q}, \omega)] \\ & + \frac{1}{4}(1 + \kappa_z^2) \text{Im}[\chi^{+-}(\vec{q}, \omega) + \chi^{*-}(\vec{q}, \omega)] \}, \quad (2) \end{aligned}$$

where k and k' are the magnitudes of the incident and scattered neutron wave vectors, $\hbar\vec{K} = \hbar\vec{k} - \hbar\vec{k}'$ is the momentum the crystal receives from the neutron, κ_z is the component of the unit scattering vector ($\vec{K}/|\vec{K}|$) along the direction of magnetization, $\hbar\omega$ is the energy gained by the crystal, γ is the gyromagnetic ratio of the neutron, m_e and e are the mass and charge of an electron, $f^\pm = [e^{\hbar\omega/kT} \pm 1]^{-1}$, $\text{Im}(\)$ means take the imaginary part, and $\vec{q} = \vec{K} - \vec{\tau}$, where \vec{q} is the reduced wave vector and $\vec{\tau}$ is the reciprocal lattice vector necessary to bring \vec{q} into the first Brillouin zone. Note that $\chi(\vec{q}, \omega)$ is periodic in $\vec{\tau}$, since the aperiodic functions of $\vec{\tau}$, the magnetic form factor $F(\vec{K})$ and the Debye-Waller factor $e^{-2W(\vec{K})}$, have been factored out of $\chi(\vec{K}, \omega)$. This factorization is a good approximation for itinerant systems, such as iron, where the d bands are narrow.

There are two types of contributions to the inelastic scattering. The χ^{zz} part of the scattering does not involve the flip of the neutron spin, and at low temperatures it is very small compared to the spin-flip cross section (because the magnet is saturated). However, it should be kept in mind that as the temperature is raised the χ^{zz} part of the scattering becomes larger, and for an isotropic ferromagnet above the transition temperature the xx , yy , and zz correlations are all equal, since there is no preferred direction remaining in the crystal. The χ^{*+} correlations give rise to the spin-flip scattering, which includes the inelastic scat-

tering of neutrons by spin waves and Stoner modes.

In order to compare theory with experiment a calculation of the susceptibility is needed. The simplest model which contains the essential features of the scattering from an itinerant electron system is based on the random-phase-approximation (RPA) to the Hubbard¹⁶ Hamiltonian. For a single band in the RPA the imaginary part of the (spin-flip) susceptibility is given by

$$\begin{aligned} \text{Im}[\chi^{-+}(\vec{q}, \omega)] \\ = \text{Im}[\chi_0^{-+}(\vec{q}, \omega)] / \{1 - I \text{Re}[\chi_0^{-+}(\vec{q}, \omega)]\}^2 \\ + \{I \text{Im}[\chi_0^{-+}(\vec{q}, \omega)]\}^2, \end{aligned} \quad (3)$$

where I is the Coulomb repulsion between electrons of opposite spin at the same site. Here $\chi_0^{-+}(\vec{q}, \omega)$ is the so-called "noninteracting" susceptibility, which is related to the single-particle excitation spectrum via

$$\chi_0^{-+}(\vec{q}, \omega) = -\frac{(g\mu_B)^2}{N} \sum_{\vec{k}} \frac{f_{\vec{k}+\vec{q}}^+ - f_{\vec{k}}^+}{\epsilon(\vec{k}+\vec{q}) - \epsilon(\vec{k}) + \Delta - \hbar\omega + i\eta}, \quad (4)$$

where Δ is the (rigid) splitting between the spin-up and spin-down energy bands $\epsilon(\vec{k})$, and the limit as $\eta \rightarrow 0^+$ is implied. The imaginary part of $\chi_0^{-+}(\vec{q}, \omega)$ is proportional to the density of (spin-flip) Stoner excitations, whose energies are given by

$$\hbar\omega_{\text{Stoner}} = \epsilon(\vec{k}+\vec{q}) - \epsilon(\vec{k}) + \Delta \quad \text{for any } \vec{k}. \quad (5)$$

For $\vec{q} = 0$, $\hbar\omega = \Delta$ for every \vec{k} , and the Stoner states are restricted to this single energy. As \vec{q} becomes nonzero, there is an increasingly larger range of band energies that satisfy Eq. (5), and the excitation energies fan out from Δ . The Stoner modes are rather diffuse in energy and hence difficult to observe by neutron-scattering techniques.

Outside the region of Stoner states, $\text{Im}[\chi_0^{-+}(\vec{q}, \omega)] \equiv 0$; so $\text{Im}[\chi^{-+}(\vec{q}, \omega)] \equiv 0$ unless $1 = I \text{Re}[\chi_0^{-+}(\vec{q}, \omega)]$. This condition is satisfied only for specific values of (\vec{q}, ω) and corresponds to the spin-wave modes. But if the spin-wave spectrum enters the region of Stoner excitations, then $\text{Im}[\chi_0^{-+}(\vec{q}, \omega)]$ is no longer zero. Equation (3) therefore no longer has a true singularity, and an intrinsic width is induced in the spin wave. The larger $\text{Im}[\chi_0^{-+}(\vec{q}, \omega)]$ is, the larger the induced width, and if $\text{Im}[\chi_0^{-+}(\vec{q}, \omega)]$ becomes large enough, the spin waves will become completely damped out. This has been interpreted as the cause of the disappearance of the spin waves in Fe and Ni at high energies.^{10, 11}

At low temperatures the band splitting is given by

$$\Delta = I(\langle n_\uparrow \rangle - \langle n_\downarrow \rangle), \quad (6)$$

where $\langle n_\uparrow \rangle - \langle n_\downarrow \rangle$ is the magnetization per atom. Thus in the simplest form of a temperature-dependent theory Δ is assumed proportional to the magnetization. As the temperature is raised, we would

therefore expect the Stoner excitations to lower in energy as Δ decreases, and as the temperature is raised through T_c the Stoner modes would extend to $\omega = 0$. In addition, the spin waves, at least in the small-wave-vector region, will decrease in energy with a renormalization that is independent of \vec{q} and proportional to the magnetization.

Quantitative calculations of $\chi(\vec{q}, \omega)$ for multiband systems are generally much more difficult to do, and the excitation spectrum can be more complicated. In general, however, all isotropic ferromagnets have a spin-wave mode at small \vec{q} with a dispersion relation^{17, 18} given by $\hbar\omega = D|\vec{q}|^2$. At elevated temperatures the theoretical problems become even more complicated. Generally, as the temperature is increased, one expects that the spin-wave energies should decrease and the linewidths increase. The Stoner excitations are also expected to lower in energy as the electron-spin correlations are reduced at higher temperatures. At long wavelengths, of course, the spin waves will become overcritically damped as the long-range order vanishes. The general behavior of $\chi(\vec{q}, \omega)$ as a function of temperature, however, is unknown.

III. EXPERIMENTAL PROCEDURES

The measurements were taken on the HB-3 triple-axis neutron spectrometer installed at the high-flux isotope reactor.¹⁹ The triple-axis technique has been discussed at length in the literature^{10, 20, 21}; so no detailed explanation will be given here. However, there are several considerations that are particularly pertinent to these experiments which should be mentioned.²²

Since the spin-wave excitations in iron extend to high energies (compared to kT), all the measurements have been taken with the incident neutron energy greater than the scattered neutron energy; so the neutrons create excitations in the sample. This is necessary because the thermal occupation factor for the high-energy spin waves is very small. A second consideration arises because the spin-wave dispersion relations in the 3d metals are very steep. This necessitates measuring the higher-energy spin waves by fixing the energies of the incident and scattered neutrons and varying \vec{K} , which is called a "constant- E " scan. This type of scan will cut directly across the dispersion surface, giving a sharp peak in the scan. The more familiar "constant- \vec{K} " scan would almost parallel the spin-wave dispersion surface. The resolution "ellipsoid" would then "drag" along the dispersion surface over a large energy range, giving a very broad distribution of scattered intensity.

Finally, in order to maximize the scattered intensity the magnetic form factor $F(\vec{K})$ needs to be kept as large as possible, which means keeping \vec{K} small. This has important practical consequences

when measuring the high-energy spin waves. In order to satisfy the momentum and energy conservation conditions for neutron scattering and also keep \vec{K} small, high scattered-neutron energies must be employed. Thus very high incident-neutron energies must be used. Scattered- and incident-neutron energies as large as 112 and 232 meV were used. At these incident energies the flux of neutrons from the reactor is greatly reduced, so that the required counting times for measurement of these spin waves are very long.

A. Equipment details

The monochromator and analyzer were beryllium crystals with a mosaic spread of 0.25° . To minimize the effects of multiple Bragg reflections in the monochromator at high incident energies, the (101) planes were oriented for reflection, whereas the (002) planes of the analyzer were generally employed. For the higher-energy spin waves, two-thirds degree (full width at half-maximum) Soller slits were used before and after the sample. For higher-resolution measurements, $\frac{1}{3}^\circ$ slits were used.²²

The samples were each mounted in a high-temperature vacuum furnace. Three calibrated thermocouples [one chromel-alumel and two Pt-Pt (10% Rh)] were spot-welded to the sample to determine the temperature. The calibration of these thermocouples was checked by increasing the resolution of the spectrometer and measuring the critical magnetic scattering as the temperature passed through the ferromagnetic transition temperature T_C . The temperature gradients across the samples were found to be less than 2°K , with a temperature stability of better than 0.5°K over a 48-h period. The temperature control of the samples was found to be more than adequate.

B. Samples

Pure iron undergoes a bcc to fcc transformation at $\sim 1180^\circ\text{K}$, which makes the growth of large single crystals very difficult. However, with the addition of ≥ 4 at.% silicon the high-temperature fcc phase is eliminated. A large single crystal can then be easily grown from the melt. The majority of the iron measurements were taken on a single crystal of ^{54}Fe (12 at.% Si) weighing 180 gm. The crystal was approximately cylindrical in shape with the [110] crystallographic axis tilted $\sim 25^\circ$ from the cylinder axis. The nuclear scattering amplitudes of ^{54}Fe and Si are equal ($b = 0.42 \times 10^{-12}$ cm); so use of the iron isotope eliminates incoherent scattering as well as reducing all the coherent nuclear scattering cross sections by a factor of ~ 5.2 ($\bar{b}_{\text{Fe}} = 0.96$). Without the large isotopically enriched crystal, accurate measurements of the high-energy spin waves would have been difficult if not impossible, particu-

larly at elevated temperatures.

Even though the silicon in Fe(Si) alloys appears to be magnetically inactive, the dilution of iron with 12% Si considerably alters the magnetic properties. The spin-wave stiffness parameter D decreases from 280 to 230 meV \AA^2 , and the transition temperature decreases from 1042 to 970°K . Thus, in order to ascertain if the magnetic behavior of the alloy is really indicative of iron, additional measurements were carried out on a single crystal of pure iron (with the natural distribution of isotopes). This sample was a cylinder weighing 23 g, with approximately the same orientation as the alloy crystal. At room temperature, the signal to noise ratio was more than seven times better for the alloy (mainly because of sample size), and this ratio increased as the temperature increased. Of course, no measurements for pure iron could be carried out above 1180°K .

IV. DATA COLLECTION AND ANALYSIS

The majority of the measurements were taken around the 110- and 002-type reciprocal-lattice points. These reciprocal-lattice points correspond to the two smallest vectors in the reciprocal lattice, and hence $F(\vec{K})$ is most favorable here. It is not practical to measure the excitations around the 000 reciprocal lattice point because the momentum and energy conservation relations cannot be satisfied for reasonable incident and scattered neutron energies.

Each scan was fitted by a least-squares procedure to a sum of Gaussian distributions (one for each peak) plus background. This should be a valid procedure if the dispersion surfaces do not deviate appreciably from planar dispersion surfaces over the extent of the (Gaussian) resolution ellipsoid, and in fact excellent fits to the data were achieved with this method. The position, integrated intensity, and width of each peak may then be extracted from the data. It was found that this was a reliable and particularly convenient method for cases when two (or more) peaks were overlapping each other, which occurred in some of the low-energy scans because of the presence of both magnons and phonons. The positions, intensities, and widths were also obtained by hand and checked with the computer results for consistency. The results agreed within experimental error. In addition, rather extensive resolution calculations were performed to determine the extent of the influence of the finite resolution of the spectrometer on the results.

A. Spin-wave linewidths

Since the scans performed were constant- E scans (varying \vec{K}), the measured widths are in units of \vec{K} rather than energy. But if the intrinsic energy widths are not too large ($\Delta E/E \ll 1$) or if the disper-

sion surface is approximately planar over the region of interest, then the energy widths can be obtained directly by

$$\Delta E = |\vec{\nabla}_{\vec{q}} \omega| \Delta q, \quad (7)$$

where $|\vec{\nabla}_{\vec{q}} \omega|$ is the slope of the dispersion surface. Above T_C , however, the intrinsic energy widths are not small. Nevertheless, Eq. (7) will still give rough estimates of the energy widths because the dispersion surface (at least at the higher energies) does not have a great deal of curvature. More reliable linewidths can be obtained by numerically folding the scattering cross section with the resolution function and fitting the calculations to the measurements. Rather extensive numerical calculations of this type have been made. The effects of the resolution and the specific assumptions used to extract the intrinsic widths of the excitations will be discussed when the linewidth data are presented.

B. Spin-wave intensities

Brockhouse *et al.*²¹ showed how the interpretation of the integrated intensities of a series of scans along a dispersion surface can be greatly simplified if the scattered neutron energy is not changed during the series of measurements and if the flux of neutrons incident upon the sample is monitored by a low-efficiency “ $1/v$ ” detector.²³ Mook and Nicklow¹⁰ have discussed in detail the interpretation of spin-wave intensities for iron taken with this experimental arrangement and using the constant- E mode of operation. If within the region where the resolution ellipsoid intersects the dispersion surface, this surface does not deviate appreciably from a plane and the variation of the scattering cross section along the dispersion surface can be ignored, then the observed integrated intensity $I(E)$ is given to a good approximation by

$$I(E) = \frac{c \sigma(\vec{K}_0, E)}{|\vec{\nabla}_{\vec{q}} \omega|} \sim \frac{(1+f^-) |F(\vec{K}_0)|^2 \chi_s(E) e^{-2W(\vec{K}_0)}}{|\vec{\nabla}_{\vec{q}} \omega|}, \quad (8)$$

where \vec{K}_0 is the value of \vec{K} at the peak position, and $\chi_s(E)$ is the spin-wave intensity. c is a complicated function of the spectrometer parameters, but does not vary from scan to scan. Mook and Nicklow found that for the types of triple-axis scans used in these measurements, Eq. (8) in fact gives a good description of the operation of the spectrometer. Precise measurements of the magnetic form factor²⁴ have been made, and the Debye-Waller factor, slope, and thermal factor are known; so the spin-wave intensities $\chi_s(E)$ can be readily extracted from the data.

The various terms in Eq. (8) occur for the following reasons. If we measure an integrated intensity $I(E)$ in a constant- E scan, then to obtain a quantity which is proportional to the “scattering strength” of a spin-wave state we need to take into

account both the density of spin-wave states which contribute to the scattering ($\sim 1/|\vec{\nabla}_{\vec{q}} \omega|$ for a constant- E scan) and the thermal occupation of these states. The magnetic form factor $F(\vec{K})$ and the Debye-Waller factor $e^{-2W(\vec{K})}$ will vary along the dispersion surface from scan to scan, although their variation is small unless the scans are done around different reciprocal-lattice points. The effects of all the other experimental factors which may vary from scan to scan (e.g., reflectivity of the monochromator and analyzer crystals, counting efficiencies of the detectors, etc.) cancel each other because of the manner in which the spectrometer is operated.

There are two points that should be clarified concerning the spin-wave intensities $\chi_s(E)$ extracted from the data. First, if the density of magnetic states per unit range of \vec{K} is a constant, and all of these states lie on the spin-wave dispersion surface, then the density of spin-wave states per unit range of energy is proportional to $1/|\vec{\nabla}_{\vec{q}} \omega|$, as for the Heisenberg model. In this case $\chi_s(E)$ would be constant as a function of energy. The spin-wave intensities presented are thus compared to this, and variations in the scattering intensity may be interpreted either in terms of a variation in the spin-wave “scattering strength” $\chi_s(E)$, or in terms of the density of states contributing to the scattering. Second, when the intensity begins to decrease rapidly at high energies, then the assumption that the scattering cross section does not vary within the resolution of the instrument is not valid, and only an “average” scattering is measured. At high spin-wave energies the energy resolution is quite coarse, and this accounts for most if not all of the smooth drop off observed. The scattering cross section itself actually drops off more rapidly than the observed spin-wave intensities indicate.

As a function of temperature there are several additional quantities in the cross section which can vary. The magnetic moment μ (analogous to S in the localized model and not $\langle S^z \rangle$) and the form factor $F(\vec{K})$ may be temperature dependent. However, measurements show^{1,25} that they have (at most) only a weak dependence on temperature, and any temperature dependence has been retained in the spin-wave intensities presented. The Debye-Waller factor $e^{-2W(\vec{K})}$ does vary with temperature, and this effect will be discussed when the data are presented.

V. EXPERIMENTAL RESULTS

Since the dispersion relations were expected to be isotropic in \vec{q} , the measurements were concentrated in the $[110]$ direction. However, enough data were obtained in the other symmetry directions to establish that the spin-wave dispersion relations, as well as the spin-wave linewidths, are isotropic

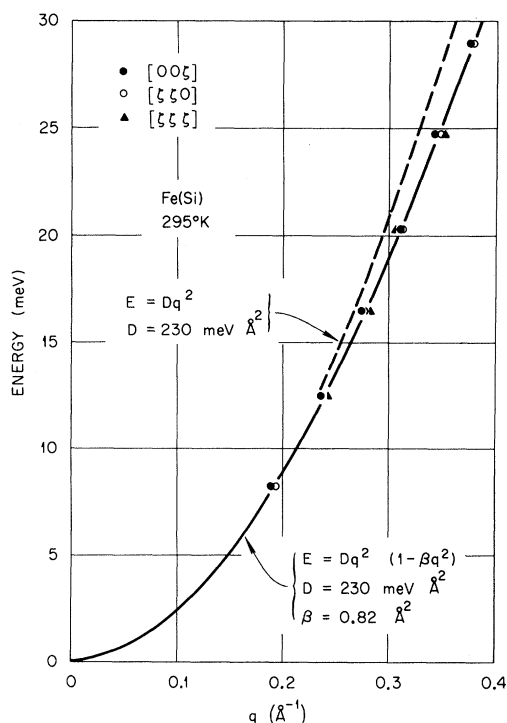


FIG. 1. Fe(12 at.% Si) room-temperature spin-wave dispersion relations at low energies in the principal symmetry directions. The dispersion relation is seen to be isotropic in \vec{q} . The zone boundary in the [100] direction corresponds to 2.20 \AA^{-1} .

in \vec{q} over the entire temperature range covered. The Stoner excitations, on the other hand, are not isotropic in \vec{q} . Because of the long counting times required to measure the high-energy spin waves, the temperature dependence of the spin-wave Stoner-mode intersection was determined only for the [110] direction in Fe(Si).

A. Room temperature

Since no triple-axis data have been reported for Fe(12 at.% Si), the room-temperature spin-wave dispersion relations were examined thoroughly. Figure 1 shows the low-energy portion of the dispersion relations for the principal symmetry directions. Measurements were taken in all three symmetry directions and around at least two different reciprocal-lattice points at all the energies shown. Within experimental error, the dispersion relations are seen to be isotropic in \vec{q} . If Eq. (1) is fitted to these data, then values of $D = 230 \pm 7 \text{ meV \AA}^2$ and $\beta = 0.82 \pm 0.20 \text{ \AA}^2$ are obtained. The errors quoted are the least-squares statistical errors. The solid curve in the figure corresponds to Eq. (1), whereas the dashed curve is just the quadratic term. These results are in reasonable agreement with the "diffraction-method" results of Antonini *et al.*,²⁶ although their results are for al-

loys of 7% and 15% Si. Our room-temperature measurements at higher energies are shown in Fig. 2.

The spin-wave intensities in the [110] direction were measured as a function of energy around both the 110- and 002-type reciprocal-lattice points and with several different scattered neutron energies. The spin-wave intensity slowly decreases with increasing energy until $\sim 100 \text{ meV}$, and then begins to decrease more rapidly (Fig. 3). This rapid decrease in intensity is interpreted as being due to damping of the spin waves by the Stoner excitations. Although exhaustive measurements like those of Mook and Nicklow¹⁰ were not carried out, it is clear that the intensity decrease occurs at a higher energy than in Fe(4 at.% Si). With consideration of the resolution used for these measurements (the energy resolution at a spin-wave energy of 120 meV is indicated in the figure by the horizontal bar) we can estimate an intersection point of $\sim 115 \text{ meV}$, which is considerably higher than the $\sim 95 \text{ meV}$ they observed. Note (Fig. 2) that the spin-wave modes exist only over about half of the Brillouin zone (the zone boundary in the [110] direction is at 1.55 \AA^{-1}).

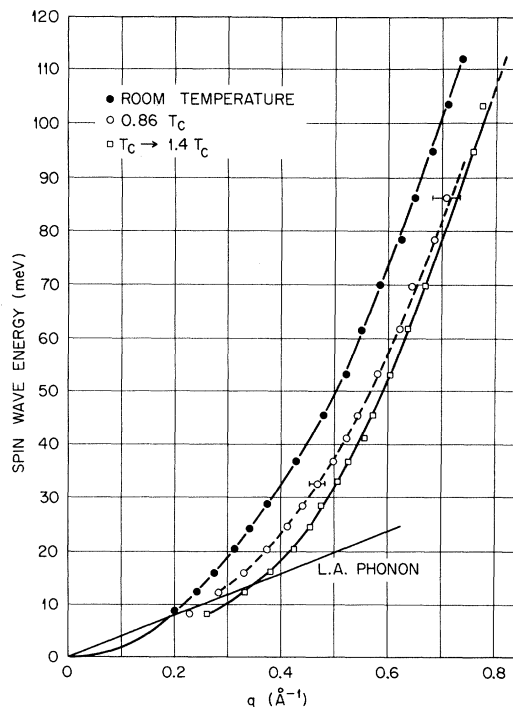


FIG. 2. Fe(Si) spin-wave spectra at a series of temperatures. The spin waves lower in energy with increasing temperature up to T_C , but outside the small-wave-vector region the dispersion relation does not renormalize to zero as $T \rightarrow T_C$, and above T_C the spin waves persist as excitations. No further renormalization is observed above T_C .

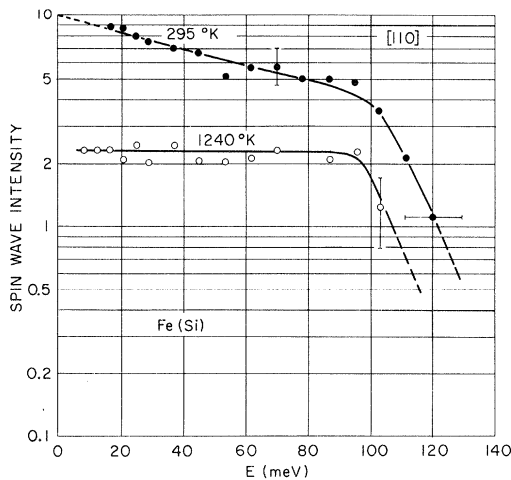


FIG. 3. Spin-wave intensity vs energy at room temperature and $1.28 T_C$ for the $[110]$ direction of Fe(Si). The rapid decrease at high energies, interpreted as the intersection of the spin-wave spectrum with the Stoner continuum, changes little, if any, with temperature. The horizontal bar at 120 meV indicates the energy resolution of the spectrometer employed at that energy.

It should be pointed out that for elevated temperatures and for the multiband case the region of Stoner states may not be as sharply defined as it is in the case of the single-band model discussed in Sec. II. The intrinsic width of the spin-wave mode is thought to be proportional to the density of Stoner states, and therefore a gradual rise in the density of Stoner states with increasing energy could explain the slow decrease in the observed spin-wave intensity (up to ~ 100 meV). However, it is not yet known theoretically how large the Stoner density of states needs to be in order to induce an appreciable intrinsic width into the spin waves, or to make them disappear altogether.

B. Temperature dependent results

The magnetic scattering from the Fe(Si) crystal was measured from room temperature through the ferromagnetic transition temperature and up to $1.4 T_C$ (1360 °K). Although the furnace could go higher in temperature, the vapor pressure of the sample would have become high enough that a significant portion of the sample would have been lost over a period of days, and this was undesirable because the ^{54}Fe isotope is very expensive. The scattering was identified as magnetic in origin both by continuously following the evolution of the scattering from low temperatures, and from the dependence of the scattering intensity on the magnetic form factor $F(\vec{K})$. Spin waves with the same \vec{q} were measured around different reciprocal lattice points and with a variety of experimental arrangements to detect any spurious scattering effects.

Figure 2 shows the temperature dependence of the spin-wave spectra for Fe(Si) in the $[110]$ direction. As the temperature is increased, the spin waves lower in energy. Outside the immediate vicinity of the origin, however, the spin waves persist as excitations up to and above T_C , with no further renormalization of the dispersion relation occurring for $T > T_C$. This behavior is in contrast to the behavior observed in the small-wave-vector region,^{8,9} where the spin waves become overcritically damped just below T_C .

If the expression $E = Dq^2$ is fitted to the data, then D is found to decrease from $230 \text{ meV}\text{\AA}^2$ at room temperature to $\sim 140 \text{ meV}\text{\AA}^2$ above T_C . About a 15% decrease in D can be expected^{6,6} in going from $T = 0^\circ\text{K}$ to room temperature, so that the overall renormalization is $\sim 50\%$. However, the fit to the data above T_C is not particularly good, and including β in the fit [Eq. (1)] results in a small value of D and a large negative value of β . An adequate fit to the dispersion relation could not be achieved without including several higher-order terms, and the curve in the figure for $T > T_C$ is just a fit to a higher-order polynomial expansion in the wave vector q . The theoretical form of the dispersion relation is not known, although it was expected that the long-wavelength spin waves should become overcritically damped just below T_C , and that $D(T)$ should follow a power law of the reduced temperature [which means that $D(T) \rightarrow 0$ as $T \rightarrow T_C$]. This behavior has been confirmed experimentally for both iron^{8,9} and nickel.²⁷

The spin-wave energies for pure iron were found to be $\sim 15\%$ higher in energy (for a given value of \vec{q}) than in the Fe(Si), and well defined spin waves were observed above T_C . Only a limited region of energy was explored, though, and of course no measurements could be taken above the solid-state transformation. The highest temperature for which measurements were taken on pure iron was 1150°K , which corresponds to $T/T_C \approx 1.1$ ($T_C = 1042^\circ\text{K}$).

Figure 3 shows the spin-wave intensity as a function of energy at room temperature ($T/T_C = 0.30$) and at $1.28 T_C$ for the $[110]$ direction of Fe(Si). It is clear that the location of the abrupt spin-wave intensity decrease at high energy changes little, if any, with temperature. This is an interesting result since the simplest theory would predict a substantial decrease in energy of the Stoner modes as the band splitting collapses with $T \rightarrow T_C$. It also appears that the slow decrease in intensity with increasing energy at room temperature is absent at high temperatures.

A few high-energy spin-wave measurements are shown in Fig. 4 for room temperature and 1240°K . It can be seen that the spin waves are broadened in \vec{q} and reduced in intensity at $1.28 T_C$, but they are still easily observable. The solid and dashed

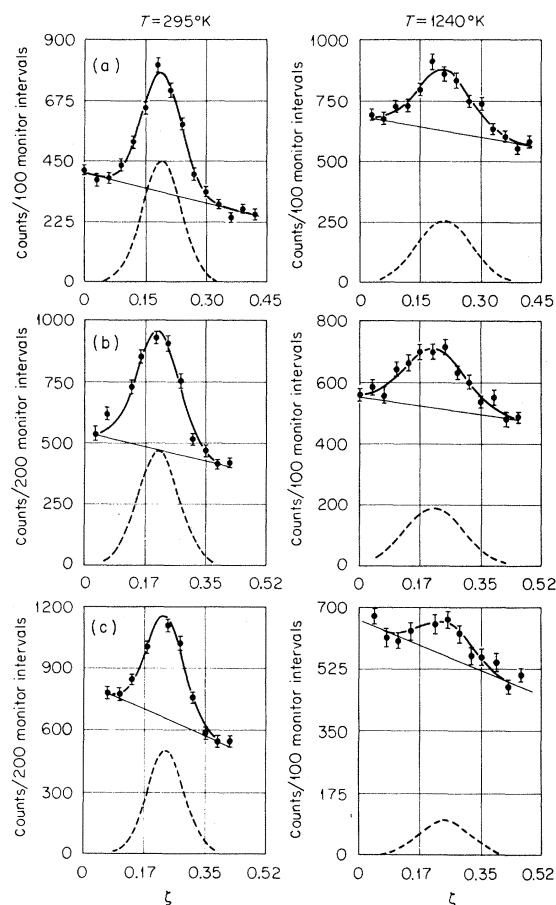


FIG. 4. Comparison of spin waves with energies of (a) 70.3 meV, (b) 95.1 meV, and (c) 103.4 meV, at room temperature and 1240 °K for $\vec{Q} = (1 + \zeta, 1 + \zeta, 0)$. The spin waves at high temperatures are reduced in intensity and broadened, but are still easily observable.

curves are the result of a least-squares fit to a Gaussian distribution plus sloping background. The sloping background in these high-energy scans is a consequence of scattering from the furnace and from air scattering, which is dependent on the scattering angle for the small angles used in these measurements.

The overall spin-wave intensities are reduced at higher temperatures, and Fig. 5 shows the temperature dependence of the spin-wave intensity for a fixed energy transfer of 29.0 meV. This temperature dependence is typical of all the spin-wave intensities, although the intensities at low energies decrease somewhat more rapidly than those at higher energies. One contribution to this decrease is the temperature dependence of the Debye-Waller factor. To check the magnitude of this effect, the intensities of a few phonon groups were also measured. Below T_C the interpretation of the temperature dependence of the phonon intensities is com-

plicated by the fact that the intensity is partly magnetic in origin, owing to magnetovibrational scattering. The phonon intensities were found to fall off fairly rapidly up to the transition temperature, but at T_C the rate of decrease abruptly changed. Above T_C , the phonon intensities decreased more slowly, in accordance with calculations of the temperature dependence of the Debye-Waller factor, while the magnon intensities decreased about four times more rapidly. This difference is most likely due to a decrease in $\chi_s(E)$, although it should be pointed out that it could partly be due to a difference in the thermal vibrational amplitudes of the electrons and nuclei.

In addition to the spin-wave positions and intensities, the intrinsic linewidths may also be extracted from the data when these widths are comparable to or larger than the resolution of the spectrometer. Figure 6 shows the observed full width at half-maximum of the spin waves at 8.27 and 29.0 meV as a function of temperature. Note that since the scans were taken with the energy transfer held constant and by varying \vec{q} , the widths are in \vec{q} rather than energy. The resolution of the spectrometer has not been removed from these widths, and the widths at room temperature may be taken as a

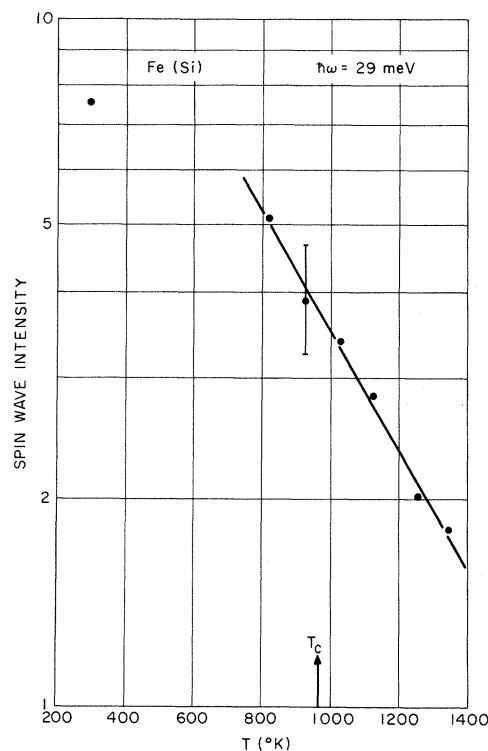


FIG. 5. Temperature dependence of the spin-wave intensity for $E = 29$ meV. The intensity decreases about four times faster than can be accounted for in terms of the Debye-Waller factor.

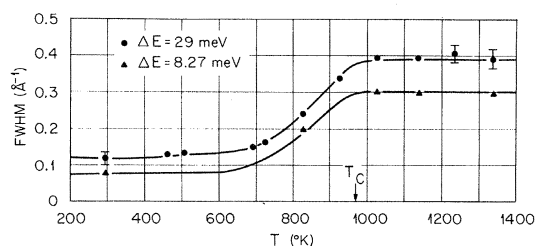


FIG. 6. Temperature dependence of the observed full width at half-maximum (in \vec{q}) for spin waves at 8.27 and 29.0 meV. The observed widths at room temperature are indicative of the resolution of the spectrometer. Solid curves are just a guide to the eye.

measure of the resolution. Detailed resolution calculations showed that the intrinsic widths at room temperature are small. As the temperature is raised to T_C , the spin waves broaden considerably, but above T_C no further broadening occurs. The solid curves in all the figures of width vs temperature are just guides to the eye. Unfortunately, theoretical results for the line shapes at large wave vectors and elevated temperatures are not available.

The widths were found to be isotropic in \vec{q} , and the majority of the measurements were therefore taken in the $[110]$ direction. Figure 7 shows several scans just below and above T_C for 8.27 meV. Two peaks are observed in each scan, the sharp peak being due to the longitudinal phonon and the broad peak being due to the spin wave. Although the presence of the phonon in the midst of the magnetic scattering is undesirable, it does afford a ready comparison of the magnetic and nuclear scattering, and it also gives an indication of the resolution of the spectrometer (the temperature broadening of the phonons is small, but measurable). Since the phonons are narrow, they may be easily separated from the magnetic scattering. The solid curves shown were obtained by a least-squares fitting procedure using two Gaussian distributions (dashed curves) plus background. If a transverse scan is made ($\vec{q} \perp \vec{Q}$), the longitudinal phonon can of course be eliminated from the scan, but then the transverse phonon appears (at a different position in $|\vec{q}|$). A variety of different scans was performed, and it was found that consistent results could be obtained by use of the fitting procedures, with a quality of fit within the statistical errors of the data. One interesting point that was observed in the low-energy data is that the positions, widths, and intensities of the phonons seem to be unaffected by the presence of the magnons. At the higher energies, of course, there are no phonons in the scans.

It should be pointed out that a peak in a constant- E scan does not necessarily imply that there is a

corresponding peak in a constant- Q scan (i.e., as a function of energy). But the width measured in \vec{q} can be related to the width in energy if the scattering is known over a sufficiently large region of (\vec{q}, ω) . For this purpose we can define a dispersion relation by the measured peak in the scattering. If this relation is approximately linear over an energy range the size of the energy width, then the energy widths can be obtained directly by multiplying the \vec{q} width by the slope of the dispersion curve [Eq. (7)]. Above T_C , however, the energy widths are large; so care must be taken in order to extract more accurate intrinsic widths from the data. Numerical convolutions of the resolution function of the spec-

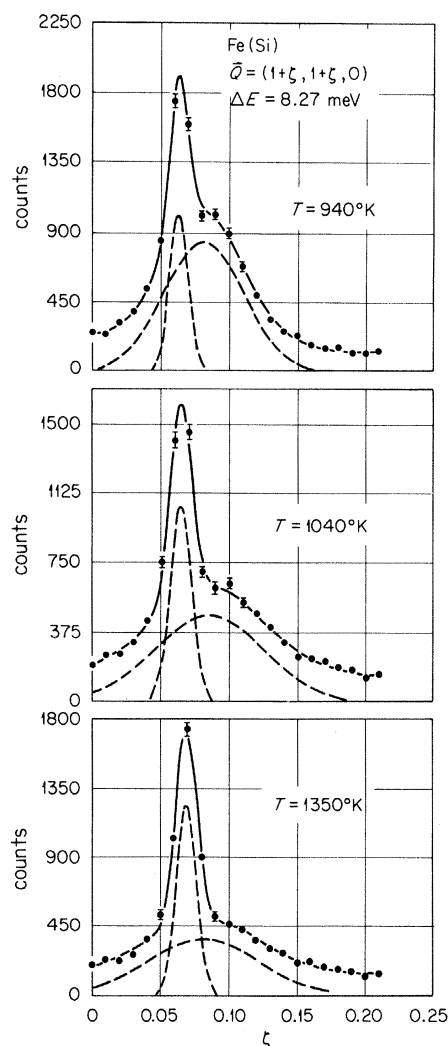


FIG. 7. Several constant- E scans at 8.27 meV above and just below the Curie temperature (970°K). The narrow peaks are LA phonons, and the broad peaks are the spin waves. Note that there does not appear to be any interaction of the spin waves with the phonons. The curves are least-squares fits of Gaussian distributions plus background to the data.

trometer with the scattering cross section have been carried out, assuming a Gaussian intrinsic-energy lineshape for the spin waves. These calculations indicate that the energy widths obtained via Eq. (7) should be reduced by no more than 10% in the worst case. These "resolution effects" are principally due to the curvature of the dispersion surface, and consequently the corrections to Eq. (7) tend to be larger at small values of the wave vector \vec{q} , where the curvature is greater. The energy widths presented have been corrected in this manner for the resolution of the spectrometer.

Since a Gaussian distribution in \vec{q} gives a good fit to the data at high temperatures, this form was assumed for the intrinsic widths. The intrinsic widths may then be obtained via $\sigma^2(\text{intrinsic}) = \sigma^2(\text{observed}) - \sigma^2(\text{resolution})$, if the curvature of the dispersion surface can be neglected. If the natural linewidths in \vec{q} are Lorentzian rather than Gaussian, then the intrinsic widths extracted from the measurements will be smaller (by about 15% for $T > T_C$) than those obtained with the Gaussian analysis, so that the Gaussian widths represent in some sense an upper limit. It should be kept in mind that the quantitative results presented for the energy widths depend on the assumption of a Gaussian linewidth, and that for the large widths present above T_C the energy lineshapes are not necessarily either Gaussian or symmetric. However, once the scattering cross section has been measured over a large region of the Brillouin zone, the energy widths [and $\chi(\vec{q}, \omega)$] can be obtained directly, without assuming any particular form for them. When this was possible, it was found that the widths estimated on the basis of the above analysis were in reasonable agreement with the actual widths. Unfortunately, the theoretical form of the energy lineshapes is not known.

Figure 8 shows the ratio of the energy width to the excitation energy as a function of temperature for $E = 37.2$ meV. The error depicted is the relative error of the energy widths and does not take into account any possible systematic errors due to

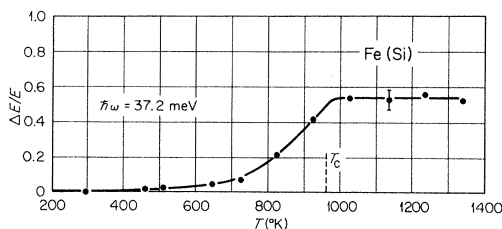


FIG. 8. Intrinsic energy width ΔE divided by energy E for $E = 37.2$ meV as a function of temperature. The energy widths rapidly increase up to T_C , but above T_C no further broadening is observed. Note that for $T > T_C$, $\Delta E/E < 1$, which has been used as the criterion for the definition of a spin-wave excitation.

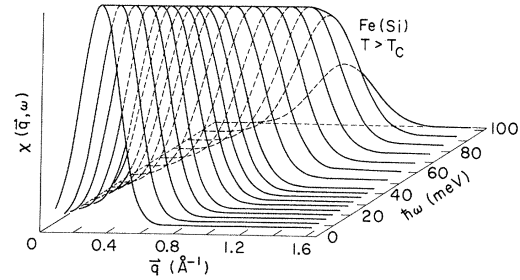


FIG. 9. Measured susceptibility $\chi(\vec{q}, \omega)$ for $T > T_C$ over the region where the "spin waves" exist ($\Delta E/E < 1$). Below ~ 8 meV, $\Delta E/E > 1$, and at high energies the susceptibility falls off because of the Stoner excitations.

the assumptions made in the analysis. The ΔE is defined in terms of the standard deviation of a Gaussian distribution. As the temperature is raised, a large intrinsic width is induced in the spin wave. Nevertheless, $\Delta E/E < 1$, which has been used as the criterion for the definition of a spin-wave excitation. Clearly these excitations do not fall into the category of overcritically damped ($\Delta E \gg E$) excitations, since for $T > T_C$ $\Delta E/E$ is less than 1 when $E \geq 8$ meV, and this ratio decreases as E increases. Just below the spin-intensity cutoff, $\Delta E/E \sim 0.33$.

Above T_C , the intrinsic width in q (or q itself) at the energy where $\Delta E/E = 1$ should give an indication of the maximum wavelength excitations that are underdamped, i. e., the dynamic correlation range. Using the (minimum) Heisenberg uncertainty relation ($\Delta q \Delta r = \frac{1}{2}$), we find that $\Delta r \sim 5 \text{ \AA}$, which can be interpreted as a "sphere of correlation" with a diameter of $\sim 10 \text{ \AA}$. The volume of this sphere is $\sim 500 \text{ \AA}^3$; so there are indeed rather long-range spin correlations above T_C . It is interesting that this range of correlation is insensitive to the temperature.

If the scattering is measured over an extended region of (\vec{q}, ω) , then the susceptibility can be obtained directly from the measurements, without assuming any particular form for it. Figure 9 shows a "three-dimensional" plot of the measured susceptibility $\chi(\vec{q}, \omega)$ above T_C over the region where the spin waves exist ($8 \leq E \leq 115$ meV). The fall off of $\chi(\vec{q}, \omega)$ at ~ 115 meV is thought to be due to damping by the Stoner excitations, and the scattering at higher energies is too small to be measured at any temperature. For $E < 8$ meV, on the other hand, the linewidth analysis showed that $\Delta E/E > 1$, and thus this scattering is predominately diffusive in nature. This "hump" of scattering (a constant- E scan still shows a peak) evolves smoothly into the critical scattering in the hydrodynamic region. The susceptibility therefore transforms continuously from the purely diffusive behavior around Γ to the propagating character at higher en-

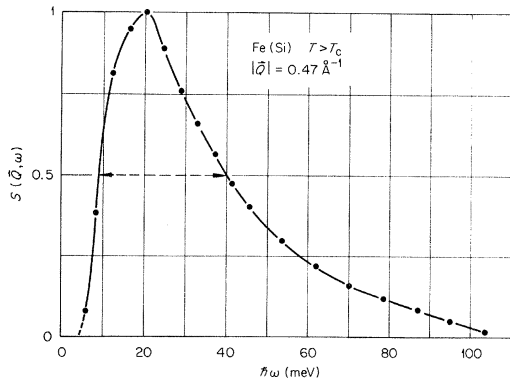


FIG. 10. Measured scattering function $S(\vec{Q}, \omega)$ corresponding to a constant- \vec{Q} scan, showing the lineshape of the spin-wave peak for $T = 1.28T_C$.

ergies and wave vectors, and we have used the criterion of $\Delta E/E = 1$ to define the "boundary" between these two regions. We have chosen to call these peaks in $\chi(q, \omega)$ at higher energies "spin waves" since the scattering closely resembles the scattering below T_C , and because of its continuous evolution in temperature with no apparent indication of T_C itself. Of course, these "spin waves" above T_C are quite broad in energy, as shown explicitly in the constant- Q scan²⁸ of Fig. 10. This plot has been obtained directly from a series of constant- E scans which contained the same points \vec{Q} , and shows an unmistakable "spin-wave" peak above T_C .

Finally, since the Fe(Si) alloy crystal has a considerable amount of silicon in it, the question arises whether the linewidths are seriously affected by the silicon. Figure 11 shows a comparison of the intrinsic linewidths for the alloy and for pure iron at an energy of 29.0 meV. The Δq is defined in terms of the standard deviation of a Gaussian distribution. Clearly, the same behavior is found for both samples, the measured linewidths being slightly smaller for the pure iron. However, the slope of the dispersion curve in pure iron is slightly larger; so the energy widths (and hence $\Delta E/E$) are essentially identical.

VI. DISCUSSION

The neutron-scattering results at low temperatures are best described by calculations of the generalized susceptibility based on band structures in which the electron correlations are treated as accurately as possible. The most extensive calculations to date are those of Cooke *et al.*,²⁹ who include a momentum-dependent spin splitting of the electronic energy bands as well as multiband effects. These calculations yield an isotropic spin-wave dispersion relation which is in quantitative agreement with the measured dispersion curve and

correctly show that the spin-wave scattering intensity abruptly dies out at ~ 100 meV. This overall agreement gives us confidence that the description of the low-temperature excitation spectrum obtained from calculations of $\chi(\vec{q}, \omega)$ based on band structure is generally correct.

Temperature-dependent calculations of $\chi(\vec{q}, \omega)$ are much more difficult to do. The only temperature-dependent calculations available are those for nickel by Lowde and Windsor,³⁰ who use the RPA "enhanced-susceptibility" expression for $\chi(\vec{q}, \omega)$ and employ a rigid (\vec{k} -independent) spin splitting of the electronic energy bands which is proportional to the magnetization. Their calculations do correctly show that away from the immediate vicinity of the critical region the susceptibility evolves smoothly through T_C . But the detailed agreement between their calculations and the experimental results for nickel^{12,13,31} is not very good. It is not really too surprising that this type of theory, which is based on a molecular-field approximation to the band structure, does not give the correct spin dynamics above T_C . This type of theory does not properly describe the strong spin fluctuations which persist above T_C . It is encouraging to see that more theoretical work is going on.³²

In comparing theory with experiment, one must keep in mind that as the temperature increases from $T = 0$, the χ^{zz} and χ^{+-} contributions to the scattering increase, and in fact above T_C all three components of the susceptibility are equal for an isotropic ferromagnet. Since there are propagating modes above T_C , there must be a propagating component of χ^{zz} as well as χ^{+-} . Thus as the susceptibility evolves from low temperatures, where the χ^{+-} part of the susceptibility dominates the scattering, the χ^{zz} part of the propagating mode must grow continuously into the spin-wave mode. Just below T_C , on the other hand, the scattering is usually divided into scattering which is predominantly spin-wave scattering (χ^{+-}) and scattering which is predominantly diffusive in nature (χ^{zz}). This diffusive scattering was expected to show up as a peak centered at $\omega = 0$, and this was clearly demonstrated

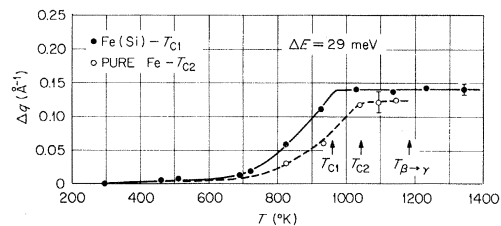


FIG. 11. Comparison of the spin-wave linewidths as a function of temperature for Fe (12 at. % Si) and pure iron. T_{C1} is the Curie temperature of the alloy, T_{C2} is the Curie temperature of pure iron, and $T_{\beta \rightarrow \gamma}$ indicates the bcc-to-fcc phase transformation of pure iron.

experimentally³³ for RbMnF_3 , which is considered to be an "ideal" Heisenberg antiferromagnet. For iron^{8,9} and nickel,²⁷ however, no central mode was observed.

These short-range spin correlations may also be important in the interpretation of other types of measurements, for example, photoemission experiments.³⁴ The measured energy distributions of photoemitted electrons at low temperatures and above T_C have been compared to the joint density of states calculated from ferromagnetic and paramagnetic band structures. This procedure eliminates from the calculations any spin correlations above T_C , which may not be justified, particularly if many-body effects are indeed crucial to the interpretation of these types of experiments.³⁵

In comparing the present results with other experiments, it should be noted that spin waves have been observed above T_N in a number of antiferromagnetic materials,^{33,36} many of which are highly anisotropic and therefore have magnetic properties of a lower dimensionality. Experiments on ferromagnets such as EuO ³⁷ and Gd ,³⁸ however, do not indicate the presence of propagating modes³⁹ above T_C . It has been suggested that perhaps the magnetic properties of iron and nickel can be explained in terms of a Heisenberg ferromagnet if the exchange interaction were extended to more distant neighbors. It would seem to be physically more appealing, though, to discuss such a long-range exchange interaction in terms of the itinerancy of the magnetic electrons. In any case, it is clear that the Heisenberg model by itself cannot describe the sharp fall off of the spin-wave intensity at any temperature.

VII. SUMMARY

The neutron inelastic-scattering technique has been used to study the temperature dependence of the magnetic excitations in iron from low temperatures to well above the ferromagnetic transition temperature. Previous measurements in the small-wave-vector region showed that the spin-wave dispersion relations renormalize to zero as $T \rightarrow T_C$, with the spin waves becoming overcritically damped just below T_C . In contrast to this behavior, the present investigation revealed that the spin waves at larger values of \vec{q} are only moderately renormalized up to T_C and persist as excitations to the highest temperature measured ($1.4 T_C$). No further renormalization is observed above T_C .

The spin-wave intensity as a function of energy has been measured for $\text{Fe}(\text{Si})$ along the $[110]$ direction. At room temperature the intensity decreases slowly with increasing energy until 100 meV, and then begins to rapidly decrease. The cause of this rapid decrease can be interpreted in terms of the band model of ferromagnetism as the intersection

of the spin-wave spectrum with the Stoner continuum of spin-flip excitations. It was expected theoretically that with increasing temperature the Stoner continuum would lower in energy, but measurements up to $1.4 T_C$ show that, within experimental error, there is no change in the location of the spin-wave intensity cutoff. The overall spin-wave intensities, however, are reduced at high temperatures. These results are in disagreement with present theoretical estimates of the generalized susceptibility at elevated temperatures.

In addition to the spin-wave energies and intensities, the linewidths were also measured. With increasing temperature, the widths of the excitations rapidly increase up to T_C , but above T_C no further broadening occurs. For $E \gtrsim 8$ meV the ratios of the energy widths above T_C to the excitation energies were found to be less than 1 ($\Delta E/E < 1$), which has been used as the criterion for the definition of a spin-wave excitation. The dynamic correlation range corresponds to a sphere with a diameter of ~ 10 Å, and this correlation range is independent of temperature over the temperature range covered above T_C . With decreasing energy the scattering evolves continuously into the critical scattering around the origin, and with increasing energy $\Delta E/E$ decreases. At energies just below the cutoff in intensity, $\Delta E/E \sim 0.33$. The spin-wave energies and linewidths were found to be isotropic in \vec{q} over the entire temperature range covered, and no interaction of the spin waves with the phonons was observed.

The overall agreement between theory and experiment at low temperatures gives us confidence that the picture of the excitation spectrum based on band structures is generally correct. Calculations of the generalized susceptibility at elevated temperatures are much more difficult to do accurately. One of the major problems with the theory stems from the use of the RPA and assuming in addition that the band splitting is proportional to the magnetization. This forces the renormalization of the dispersion relations with temperature (at least at small \vec{q}) to be independent of \vec{q} and substantially lowers the region of Stoner excitations, which is contrary to experiment. The electron correlations at elevated temperatures will need to be incorporated into the theory in a more realistic manner in order to produce the strong short-range spin correlations necessary to support collective excitations above the ferromagnetic transition temperature. Clearly more theoretical effort will be needed in order to bring theory into agreement with experiment at elevated temperatures.

ACKNOWLEDGMENTS

The author would like to express his deepest ap-

preciation to Dr. H. A. Mook, Dr. R. M. Nicklow, Dr. J. F. Cooke, and Dr. M. K. Wilkinson of the Oak Ridge National Laboratory and Dr. H. A. Gersch of the Georgia Institute of Technology for the expert professional guidance and personal encouragement given the author during the course of his doctoral dissertation. The many helpful dis-

cussions with H. G. Smith, H. L. Davis, N. Wakabayashi, W. C. Koehler, R. M. Moon, J. W. Cable, and H. R. Child and the valuable technical assistance of Mr. J. L. Sellers are also gratefully acknowledged. The author would also like to thank D. L. Holcomb and A. C. Kimbrough for the design and construction of the furnace used in these studies.

*Research sponsored by the U. S. Atomic Energy Commission under contract with Union Carbide Corporation.

†Oak Ridge Associated Universities Graduate Fellow. This work comprises a portion of a Ph. D. thesis in physics submitted to the Georgia Institute of Technology.

‡Present address: Physics Department, Brookhaven National Laboratory, Upton, Long Island, New York 11973.

¹A thorough discussion of the experimental and theoretical considerations pertaining to the "localized" and "itinerant" viewpoints as well as extensive references to the literature are given in the review by C. Herring [in *Magnetism*, edited by G. T. Rado and H. Suhl (Academic, New York, 1967), Vol. 4].

²For a recent discussion see, for example, G. Lonzarich and A. V. Gold, *Can. J. Phys.* **52**, 694 (1974), and references therein.

³L. Passell, K. Blinowski, T. Brun, and P. Nielsen, *Phys. Rev.* **139**, A1866 (1965).

⁴D. Bally, B. Grabcev, A. M. Lungu, M. Popovici, and M. Totia, *J. Phys. Chem. Solids* **28**, 1947 (1967).

⁵G. Shirane, V. J. Minkiewicz, and R. Nathans, *J. Appl. Phys.* **39**, 383 (1968).

⁶M. W. Stringfellow, *J. Phys. C* **1**, 950 (1968).

⁷An extensive list of references is given in a thesis by J. W. Lynn [Georgia Institute of Technology (unpublished)].

⁸M. F. Collins, V. J. Minkiewicz, R. Nathans, L. Passell, and G. Shirane, *Phys. Rev.* **179**, 417 (1969). See also Ref. 5.

⁹S. Boronkay and M. F. Collins, *Int. J. Magn.* **4**, 205 (1973).

¹⁰H. A. Mook and R. M. Nicklow, *Phys. Rev. B* **7**, 336 (1973); H. A. Mook and R. M. Nicklow, *J. Phys. (Paris)* **32**, 1177 (1971).

¹¹H. A. Mook, R. M. Nicklow, E. D. Thompson, and M. K. Wilkinson, *J. Appl. Phys.* **40**, 1450 (1969).

¹²H. A. Mook, J. W. Lynn, and R. M. Nicklow, *Phys. Rev. Lett.* **30**, 556 (1973).

¹³H. A. Mook, J. W. Lynn, and R. M. Nicklow, *AIP Conf. Proc.* **18**, 781 (1974); J. W. Lynn, *Bull. Am. Phys. Soc.* **19**, 231 (1974).

¹⁴Since the orbital moment ($\sim 5\%$ for iron) is not expected to introduce any new features into the excitation spectrum for the region of interest, the discussion is simplified to considering only the spin contribution to the magnetic scattering. In addition, the present experiments were performed with an unpolarized neutron beam incident upon an unmagnetized sample.

¹⁵A thorough discussion of thermal-neutron scattering, with particular attention to itinerant electron systems, is given by W. Marshall and S. W. Lovesey [*Thermal Neutron Scattering* (Oxford U. P., London, 1971)]. See

also T. Izuyama, D. Kim, and R. Kubo, *J. Phys. Soc. Jpn.* **18**, 1025 (1963); J. B. Sokoloff, *Phys. Rev.* **180**, 613 (1969); J. F. Cooke, *Phys. Rev. B* **7**, 1108 (1973).

¹⁶J. Hubbard, *Proc. R. Soc. A* **276**, 238 (1963).

¹⁷T. Izuyama, *Phys. Rev. B* **5**, 190 (1972).

¹⁸At least in cases where antisymmetric exchange vanishes. R. L. Melcher, *Phys. Rev. Lett.* **30**, 125 (1973).

¹⁹M. K. Wilkinson, H. G. Smith, W. C. Koehler, R. M. Nicklow, and R. M. Moon, in *Neutron Inelastic Scattering* (IAEA, Vienna, 1968), Vol. II, p. 253.

²⁰M. J. Cooper and R. Nathans, *Acta Crystallogr.* **23**, 357 (1967).

²¹B. N. Brockhouse, L. N. Becka, K. R. Rao, and A. D. B. Woods, in *Second Symposium on Inelastic Scattering of Neutron in Solids and Liquids* (IAEA, Vienna, 1963), Vol. II, p. 23.

²²Further details can be found in the thesis by J. W. Lynn (Ref. 7).

²³For the range of incident neutron energies up to ~ 200 meV, the uranium fission detector employed as a monitor has a cross section proportional to $1/v$. This monitor-efficiency factor cancels the factor k'/k in the neutron cross section. At higher incident energies a small correction has to be applied. The monitor counting rate also has to be corrected for incoherent scattering from the monochromator, which can be appreciable at high incident-neutron energies. This has been corrected by setting the monochromator crystal off the Bragg reflection and determining the counting rate of the monitor. At the highest incident energies used, this amounted to no more than 5% of the total flux, and the spin-wave intensities have been corrected for it.

²⁴C. G. Shull and Y. Yamada, *J. Phys. Soc. Jpn.* **17**, Suppl. B III, 1 (1962); C. G. Shull, in *Electronic Structure and Alloy Chemistry of the Transition Elements*, edited by P. A. Beck (Wiley, New York, 1963), p. 69; C. G. Shull and H. A. Mook, *Phys. Rev. Lett.* **16**, 184 (1966); J. Moss and P. J. Brown, *J. Phys. F* **2**, 358 (1972).

²⁵R. C. Maglic, *AIP Conf. Proc.* **5**, 1420 (1971).

²⁶B. Antonini, F. Menzinger, A. Paoletti, and A. Tucciaroni, *Phys. Rev.* **178**, 833 (1969).

²⁷V. J. Minkiewicz, M. F. Collins, R. Nathans, and G. Shirane, *Phys. Rev.* **182**, 624 (1969).

²⁸For a constant- \vec{Q} scan $S(\vec{Q}, \omega)$ is the same (within a constant) as $\text{Im}[\chi(\vec{Q}, \omega)]$, except that $S(\vec{Q}, \omega)$ contains the Bose thermal factor.

²⁹J. F. Cooke, J. W. Lynn, and H. L. Davis (unpublished).

³⁰R. D. Lowde and C. G. Windsor, *Adv. Phys.* **19**, 813 (1970), and references therein.

³¹J. W. Lynn and H. A. Mook (unpublished).

³²L. C. Bartel, *Phys. Rev. B* **8**, 5316 (1973); J. B. Sokoloff, *Phys. Rev. Lett.* **31**, 1417 (1973); B. H. Brandow, *Bull. Am. Phys. Soc.* **19**, 370 (1974).

³³R. Nathans, F. Menzinger, and S. J. Pickart, *J. Appl.*

- Phys. 39, 1237 (1968); A. Tucciarone, H. Y. Lau, L. M. Corliss, A. Delapalme, and J. M. Hastings, Phys. Rev. B 4, 3206 (1971); D. H. Saunderson, C. G. Windsor, G. A. Briggs, M. T. Evans, and E. A. Hutchison, in *Neutron Inelastic Scattering* (IAEA, Vienna, 1972), p. 639.
- ³⁴C. S. Fadley and D. A. Shirley, Phys. Rev. Lett. 21, 980 (1968); A. J. McAlister, J. R. Cuthill, R. C. Dobbryn, and M. L. Williams, Phys. Rev. Lett. 29, 179 (1972).
- ³⁵See, for example, P. W. Anderson, Philos. Mag. 24, 203 (1971); S. Doniach, AIP Conf. Proc. 5, 549 (1972); J. A. Hertz and K. Aoi, Phys. Rev. B 8, 3252 (1973); W. Baltensperger, Helv. Phys. Acta 45, 203 (1973).
- ³⁶See, for example, S. K. Sinha, S. H. Liu, L. D. Muhlestein, and N. Wakabayashi, Phys. Rev. Lett. 23, 311 (1969); P. A. Fleury, Phys. Rev. 180, 591 (1969); J. Skalyo, Jr., G. Shirane, R. J. Birgeneau, and H. J. Guggenheim, Phys. Rev. Lett. 23, 1394 (1969); P. A. Fleury and H. J. Guggenheim, Phys. Rev. Lett. 24, 1346 (1970); M. P. Schulhof, R. Nathans, P. Heller, and A. Linz, Phys. Rev. B 4, 2254 (1971); M. J. Hutchings, G. Shirane, R. J. Birgeneau, and S. L. Holt, Phys. Rev. B 5, 1999 (1972).
- ³⁷L. Passell, J. Als-Neilsen, and O. W. Dietrich, in *Neutron Inelastic Scattering* (IAEA, Vienna, 1972), p. 619; C. J. Glinka, V. J. Minkiewicz, L. Passell, and M. W. Shafer, AIP Conf. Proc. 18, 1060 (1974).
- ³⁸H. R. Child and R. M. Nicklow, Bull. Am. Phys. Soc. 19, 206 (1974).
- ³⁹This is also true of other heavy rare-earth metals; R. M. Nicklow (private communication).